



Article

# Evaluating the Cytotoxicity of Functionalized MWCNT and Microbial Biofilm Formation on PHBV Composites

Thaís Larissa do Amaral Montanheiro <sup>1,2,\*</sup> , Vanessa Modelski Schatkoski <sup>1</sup> ,  
Denisse Esther Mallaupoma Camarena <sup>3,4</sup> , Thais Cardoso de Oliveira <sup>5</sup>, Diego Morais da Silva <sup>6</sup> ,  
Mariana Raquel da Cruz Vegian <sup>6</sup>, Luiz Henrique Catalani <sup>3</sup> , Cristiane Yumi Koga-Ito <sup>6</sup> ,  
and Gilmar Patrocínio Thim <sup>1</sup>

- <sup>1</sup> Plasma and Processes Laboratory, Technological Institute of Aeronautics, São José dos Campos 12228-900, SP, Brazil; modelski.vanessa@gmail.com (V.M.S.); gilmar@ita.br (G.P.T.)
  - <sup>2</sup> Mechanical Engineering Department, Technological Institute of Aeronautics, São José dos Campos 12228-900, SP, Brazil
  - <sup>3</sup> Laboratory of Polymeric Biomaterials, Department of Fundamental Chemistry, Institute of Chemistry, University of São Paulo, São Paulo 05508-000, SP, Brazil; denisse23uni@usp.br (D.E.M.C.); catalani@usp.br (L.H.C.)
  - <sup>4</sup> Department of Clinical and Toxicological Analysis, School of Pharmaceutical Sciences, University of São Paulo, São Paulo 05508-000, SP, Brazil
  - <sup>5</sup> Fundamental Sciences Division, Technological Institute of Aeronautics, São José dos Campos 12228-900, SP, Brazil; thaiscardoso@me.com
  - <sup>6</sup> Department of Environmental Engineering and Sciences, Oral Health Graduate Program, São José dos Campos Institute of Science and Technology, São Paulo State University (UNESP), São José dos Campos 12245-000, SP, Brazil; diego.m.silva@unesp.br (D.M.d.S.); mariana.vegian@unesp.br (M.R.d.C.V.); cristiane.koga-ito@unesp.br (C.Y.K.-I.)
- \* Correspondence: thais@ita.br



**Citation:** Montanheiro, T.L.d.A.; Schatkoski, V.M.; Camarena, D.E.M.; de Oliveira, T.C.; da Silva, D.M.; Vegian, M.R.d.C.; Catalani, L.H.; Koga-Ito, C.Y.; Thim, G.P. Evaluating the Cytotoxicity of Functionalized MWCNT and Microbial Biofilm Formation on PHBV Composites. *C* **2024**, *10*, 33. <https://doi.org/10.3390/c10020033>

Academic Editors: Giuseppe Cirillo and Stefano Bellucci

Received: 27 January 2024

Revised: 18 March 2024

Accepted: 27 March 2024

Published: 31 March 2024



**Copyright:** © 2024 by the authors. Licensee MDPI, Basel, Switzerland. This article is an open access article distributed under the terms and conditions of the Creative Commons Attribution (CC BY) license (<https://creativecommons.org/licenses/by/4.0/>).

**Abstract:** This study focuses on the cytotoxic evaluation of functionalized multi-walled carbon nanotubes (MWCNT) and microbial biofilm formation on poly(3-hydroxybutyrate-co-3-hydroxyvalerate) (PHBV) nanocomposites incorporating MWCNTs functionalized with gamma-aminobutyric acid (GABA) and carboxyl groups. The materials were characterized for cytotoxicity to fibroblasts and antimicrobial effects against *Escherichia coli*, *Staphylococcus aureus* and *Candida albicans*. The functionalization of MWCNTs was performed through oxidation (CNT-Ox) and GABA attachment (CNT-GB). The PHBV/CNT nanocomposites were produced via melt mixing. All MWCNT suspensions showed non-toxic behaviors after 24 h of incubation (viability higher than 70%); however, prolonged incubation and higher concentrations led to increased cytotoxicity. The antibacterial potential of PHBV/CNT nanocomposites against *S. aureus* showed a reduction in biofilm formation of 64% for PHBV/CNT-GB and 20% for PHBV/CNT-Ox, compared to neat PHBV. Against *C. albicans*, no reduction was observed. The results indicate promising applications for PHBV/CNT nanocomposites in managing bacterial infections, with GABA-functionalized CNTs showing enhanced performance.

**Keywords:** carbon nanotube; poly(3-hydroxybutyrate-co-3-hydroxyvalerate); nanocomposite; cytotoxicity; biofilm formation

## 1. Introduction

Carbon nanotubes (CNTs) are a carbon allotrope that has been extensively studied in different areas such as engineering, medicine, biology, and chemistry. Their unique features include high mechanical resistance, electrical and optical properties. Additionally, CNTs are hydrophobic in nature and can be functionalized to suit specific applications [1–5].

Concerning the biomedical field, the hydrophobic nature of CNTs plays a major role in reducing their biocompatibility due to their ability to damage the cell membrane, cause oxidative stress and mitochondrial activity modifications, and alter intracellular metabolic

routes, among others [6]. However, their interaction with the biological environment relies on the morphology, structure, and purity of CNTs, which are determined by the preparation, purification, and functionalization methods employed during their synthesis [6–8]. Some recent studies even mention that it is possible to use CNTs in tissue engineering, as they are biocompatible and present a lack of toxicity when interacting with cells; however, their behavior when used for in vivo applications is not fully understood [9,10]. Due to these properties, CNTs have been incorporated into polymer matrices to improve their effective properties and introduce additional functionality, such as better mechanical and electrical properties and improved cellular adhesion [11–14].

Poly-3-hydroxybutyrate-co-3-hydroxyvalerate (PHBV) is a biodegradable and biocompatible polymer, making it suitable for medical applications where biocompatibility is essential [15,16]. It can be used in various applications, including with certain instruments, and for medical implants, drug delivery systems, sutures, and tissue engineering scaffolds [17]. Its properties make it a valuable material for creating environmentally friendly and safe medical products. The main drawback of using PHBV is its limited thermal and mechanical properties compared to some synthetic polymers, which may restrict its use in specific applications that demand high strength or durability [15]. However, ongoing research and advancements in biopolymer technology aim to address these limitations and improve the cost-effectiveness and performance of PHBV, making it a more viable option for various applications in the future.

Research has explored the creation of PHBV nanocomposites containing various nanoparticles, such as cellulose nanocrystals [18–20], carbon nanotubes (CNT) [21–24], inorganic nanoparticles [25,26], and other nanomaterials [13]. These alternatives enhance their thermal and mechanical properties, making them suitable for specific applications.

CNTs have been highlighted as a candidate due to their antimicrobial effects when in direct contact with microorganisms. CNTs can inhibit bacterial adhesion and biofilm formation due to their effects on the microbial cell wall or membrane [27].

The demand for PHAs in the biomedical industry has increased globally in post-COVID pandemic era [28]. PHBV is an environmentally friendly and attractive candidate for replacing petroleum-based polymers in many applications. Disposable products such as syringes and blood bags, materials needed for surgical operations such as sutures, adhesives, and sealants, cardiovascular patches, nerve guides, and surgical meshes with poly-3-hydroxybutyrate (PHB) coating for hernioplasty surgery are some of the advanced applications of polyhydroxyalkanoate (PHA) and its blends [28,29].

However, the lack of antimicrobial activity of this biopolymer restricts its potential applications. As far as medical devices are concerned, microbial adhesion on the surface often results in severe infections and material failure. Additionally, in the event of biofilm formation, the metabolic activity of the attached microorganisms can trigger biodegradation by releasing extracellular enzymes [30–32]. Therefore, inhibiting the initial interactions between the polymer's surface and microorganisms plays a crucial role in shaping the material's long-term destiny and durability.

To address this issue, incorporating additives with established antimicrobial properties is seen as a viable approach to creating biodegradable antimicrobial materials. Thus, several researchers have investigated the antimicrobial effects of composites containing CNTs. A recent study by Vagos et al. (2020) [33] evaluated the thermal and electrical properties, as well as the bacterial adhesion, of pristine and chemically functionalized CNTs incorporated into poly(dimethylsiloxane) (PDMS). CNTs were oxidized with nitric acid ( $\text{HNO}_3$ ). The introduction of the CNTs in the PDMS matrix yielded reduced bacterial adhesion compared to PDMS alone. Similarly, Goodwin et al. (2015) [34] showed the antimicrobial effect of oxidized multi-wall CNTs and poly- $\epsilon$ -caprolactone (PCL) composites against *P. aeruginosa*. CNTs accumulated on the surface as the polymer was degraded, causing an antimicrobial effect on the composite material. Therefore, the presence of CNTs in polymer matrices can promote an increase in the antimicrobial properties of these materials, in addition to promoting an improvement in the physicochemical properties of the polymer.

The best properties that second-phase particles can offer to polymeric composites are only achieved through the optimal dispersion of this type of material in the matrix. The functionalization of fillers is an essential tool used to improve the dispersion and the interaction between the nanoparticle and the matrix.

Different strategies have been proposed to functionalize carbon nanotubes (CNTs) to achieve good dispersion and compatibility in polymeric matrices. For example, using aggressive acids such as HNO<sub>3</sub> to introduce oxygen groups with a negative charge can separate tube aggregation by reducing the Van der Waals forces between them [35]. This, in turn, enhances their dispersion within the polymer matrix. Moreover, surface functionalization can facilitate effective intracellular uptake and enhance the potential for attaching various functional groups to the surfaces of CNTs in biomedical applications.

In previous work [3], we reported the possibility of functionalizing oxidized CNTs (CNT-Ox) with gamma-aminobutyric acid (GABA) (CNT-GB) to improve the compatibility between CNTs and PHBV. GABA is a small organic compound containing amino and carboxylic functional groups, which serves as a prominent inhibitory neurotransmitter within the central nervous systems of humans [36,37]. Talodthaisong et al. (2021) [36] showed the effectiveness of ZnO nanoparticles decorated with  $\gamma$ -aminobutyric acid (GABA) against *E. coli* and *S. aureus*.

So, due to the non-toxicity of GABA and its bi-functionality, we utilize it in this work to functionalize MWCNT, aiming to improve the interaction between MWCNT and the PHBV matrix. The cytotoxicity of functionalized MWCNTs was evaluated at different concentrations, and their effects against bacterial and fungal species when included in the PHBV matrix were evaluated.

## 2. Materials and Methods

Poly(3-hydroxybutyrate-co-3-hydroxyvalerate) (PHBV) was supplied by PHB Industrial (Brazil), with a molar mass (Mw) of 159,000 g mol<sup>-1</sup> with 15% hydroxyvalerate units (HV). MWCNTs with a minimum purity of 95% by mass, a diameter in the range of 20 to 30 nm, and a length in the range of 10 to 30  $\mu$ m were supplied by Nanostructured & Amorphous Materials, Inc. with specification #1229Y.  $\gamma$ -aminobutyric acid (GABA) was purchased from Sigma-Aldrich (St. Louis, MO, USA) with a minimum purity of 99%. Nitric acid 65% P.A. and dimethyl sulfoxide (DMSO) P.A. were purchased from Neon Comercial (Suzano, SP, Brazil), and chloroform was derived from Synth (Diadema, SP, Brazil). All materials were used as received.

Fibroblasts were provided by the Laboratory of Clinical Cytopathology Cell Bank, Faculty of Pharmaceutical Sciences, University of São Paulo, Brazil. Fibroblasts were isolated from the foreskins of infants and children aged up to 10 years undergoing circumcision surgery at the University Hospital of the University of São Paulo (Brazil). The rules of the local ethics committee were followed under registration number CEP-HU/USP 943/09, SISNEP CAAE 0062.0.198.000-9, as reported by Immich and collaborators [38]. The primary cells were cultured in Dulbecco's modified Eagle medium (DMEM—Powder, High Glucose, Gibco<sup>®</sup>, Life Technologies, Carlsbad, CA, USA) supplemented with 10% *v/v* fetal bovine serum (FBS, Gibco, Life Technologies, USA) and maintained in an incubator at 37 °C with 5% CO<sub>2</sub>. The culture medium was supplemented with ampicillin (Sigma-Aldrich, DE, USA) and streptomycin sulfate (Gibco<sup>®</sup>, Life Technologies, USA).

For the biofilm formation assay, Tryptone Soy Broth (TSB) from OXOID, Brain Heart Infusion Agar from KASVI, Brain Heart Infusion Broth from KASVI, Sabouraud Dextrose Agar Eur. Pharma from KASVI, Sodium Chloride P.A. A.C.S from Synth, and RPMI—1640 Medium from Sigma-Aldrich were used.

### 2.1. Functionalization of Carbon Nanotubes

#### 2.1.1. Oxidation of Carbon Nanotubes (CNT-Ox)

The CNT was functionalized with carboxyl and hydroxyl groups through an orientation reaction with nitric acid using a previously reported protocol [2]. CNT was placed in

round bottom flasks with  $6 \text{ mol L}^{-1}$   $\text{HNO}_3$  solution, and the flask was left under reflux for 5 h at  $120^\circ\text{C}$ . After shipping, the samples were centrifuged and washed with deionized water until residual acid was removed and a neutral pH was obtained. The samples were subsequently frozen and lyophilized.

### 2.1.2. Functionalization of Carbon Nanotubes with Gamma-Aminobutyric Acid (NTC-GB)

Functionalization with GABA was performed in DMSO at  $120^\circ\text{C}$ , as described in our previous study [3]. The DMSO was previously heated to  $120^\circ\text{C}$ ; then, the Ox-CNT was added under refrigeration on a heating plate, forming a suspension. Then, GABA was slowly incorporated into the suspension in a 1:1 mass ratio (mGABA:mNTC-Ox). The system was maintained at  $120^\circ\text{C}$  under permanence for 10 h. After the reaction period, the CNT-GB was filtered and washed with deionized water to remove DMSO and unreacted GABA.

### 2.2. Production of PHBV/CNT Nanocomposites

PHBV/CNT nanocomposites were produced according to our previously published paper [22], and as described in the following. PHBV/CNT nanocomposites containing 0.5 wt. % of CNT, CNT-Ox, and CNT-GB were fabricated via melt mixing, followed by hot compression molding. Neat PHBV and the nanocomposites PHBV/CNT, PHBV/CNT-Ox, and PHBV/CNT-GB underwent processing in a high-speed mixer (DRAIS mixer manufactured by MH Equipamentos Ltda., São Paulo, Brazil, model MH50-H) rotating at 3000 rpm, with a mixing chamber capacity of 65 g of material. The steps of mixing, melting, and homogenization of the samples occurred due to the high friction generated between the rotor and the material. The PHBV mass was previously oven-dried for 4 h at  $40^\circ\text{C}$ . After 1 min of mixing, the homogenized composites were collected and pressed in a hydropneumatic press (MH Equipamentos Ltda., São Paulo, Brazil, model PR8HP) into 3.2 mm thick plates with dimensions of length 63.5 mm, width 12.7 mm, and thickness 3.28 mm. The pressing was conducted at  $200^\circ\text{C}$  using a pressure of 5 bar for 3 min, followed by cooling for 2 min.

### 2.3. In Vitro Cytotoxicity Assay

The cytotoxicity was verified through the biological response of human fibroblast cells in vitro, according to ISO 10993-5 (ISO/EN10993-5 2009) [39]. At first, extracts of the samples were prepared, followed by incubation with the fibroblasts and the determination of final cell viability by 3-(4,5-dimethylthiazol-2-yl)-2,5-diphenyltetrazolium bromide (MTT, 98%, Sigma-Aldrich, St. Louis, MO, USA).

#### 2.3.1. Preparation of the Extracts

For extracting the sample, the same cultivation media used for the fibroblast was used—Dulbecco's modified Eagle's medium (DMEM) and 10% fetal bovine serum (SFB). The samples, named CNT, CNT-ox, and CNT-GB, were autoclaved to certify their sterility. The extracts were diluted from a 10 mg/mL extract incubated at  $37^\circ\text{C}$  and 5%  $\text{CO}_2$  at 24 h, resulting in extracts at concentrations 0 (control sample free of CNTs), 1, 5, 10, 50, 100, 500, and 1000  $\mu\text{g/mL}$ . These extracts were used as the cultivation medium for monolayer cells at 80% confluence (described in Section 2.3.2). Furthermore, as seen in the Section 3, the expansion of CNTs concentration in the extract was due to the lack of response in the cytotoxicity assay with extracts from 1 to 1000  $\mu\text{g/mL}$ . Then, the concentration interval was expanded, and extracts from 1 to 6000  $\mu\text{g/mL}$  of CNTs were evaluated. These samples were prepared with 1 mg to 30 mg of CNTs suspended in the media and maintained for 1, 4, and 6 days at  $37^\circ\text{C}$  and 5%  $\text{CO}_2$ . Afterward, the extracts were used as a cultivation medium for monolayer cells at 80% confluence.

### 2.3.2. Cellular Incubation

In a 96-well plate,  $10^4$  cells were seeded and maintained at incubation with DMEM, 10% SFB at 37 °C, and 5% CO<sub>2</sub>. Then, after 24 h incubation, the cells achieved 80% confluence. In such cellular conditions, the cell monolayers were exposed to 100 µL of the prepared extracts, as described in Section 2.3.1. The CNTs cell extracts were maintained at incubation for 24 h (37 °C and 5% CO<sub>2</sub>), followed by the cell viability assay.

### 2.3.3. MTT Assay

After 24 h of the cells' exposure to the CNTs extract, the cultivation medium was removed from the 96-well plate, followed by the addition of 50 µL of MTT (1 mg/mL) in each well; the samples were maintained in incubation at 37 °C and 5% CO<sub>2</sub> for 2 h. After the MTT solution was removed, 100 µL DMSO was added, and the plates were kept from light while being agitated for 2 h. Then, each plate was transferred to a microplate reader (Infinite M200PRO NanoQuant, TCAN, Switzerland), and the optic density (DO) was measured at 570 nm. The cell viability (VR) was calculated by the relative viability following Equation (1):

$$VR (\%) = \frac{[OD]_{\text{extract}} \times 100}{[OD]_0} \quad (1)$$

where  $[OD]_{\text{extract}}$  is the value read from the measurement of the well plate exposed to the CNTs extracts, and  $[OD]_0$  is the value from the control sample (0 µg/mL). Applying this equation, the lower the VR value, the higher the cytotoxic potential from the tested sample. Moreover, if the viability is 70% lower than the value obtained for the control sample, there is cytotoxic potential.

The experiments were conducted using biological triplicates using three techniques. Analysis of variance (ANOVA) and Dunnett test (95% confidence interval) were performed in the Minitab<sup>®</sup> Statistical Software version 20.3 (Minitab, LLC; State College, PA, USA) to assess the difference between the control and CNT samples. The graphs were elaborated in GraphPad Prisma 8 (GraphPad, San Diego, CA, USA).

## 2.4. Antibiofilm Activity Test

The biofilm was grown on the nanocomposite sample surface (X mm × Y mm ø). All the samples were autoclaved (121 °C for 20 min), conditioned in a medical-grade sheet. The microbial strains used in the tests were *Staphylococcus aureus* (ATCC 6538), *Escherichia coli* (ATCC 10799), and *Candida albicans* (ATCC 18804). All the microorganisms were kept in BHI broth supplemented with 20% glycerol in a –80 °C freezer until the experiment. The fresh cultures were obtained by plating the bacteria on the Brain Heart Infusion (BHI) agar and *C. albicans* on the Sabouraud Dextrose (SD) agar. The Petri dishes were incubated for 24 h at 37 °C. Then, standardized suspensions containing  $1 \times 10^7$  CFU/mL of each microorganism were obtained with a spectrophotometer (AJX-1600 Espectofotômetro AJ Micronal) in physiological solution (NaCl 0.9%). The following parameters of wavelength and optical density were used: *Staphylococcus aureus* (490 nm and 0.111), *Escherichia coli* (530 nm and 0.020), and *Candida albicans* (530 nm and 0.138). Then, the samples were placed inside microtubes (500 mL size) containing 450 µL liquid culture medium, this being Tryptic Soy broth (TSB) added to *S. aureus*, BHI broth added to *E. coli*, and RPMI 1640 supplemented with 2% glucose added to *C. albicans*. Afterward, 50 µL was added to each microtube and vortexed for 40 s. The microtubes were vertically positioned in microtube support and then incubated under 140 rpm for 24 h at 37 °C.

After incubation, the culture medium was removed and the sample was washed once with a physiological solution and transferred with the aid of sterile tweezers to a microtube containing 500 µL of physiological solution. The microtubes were then vortexed for 3 min in order to recover the microorganisms from the surface of the samples. A serial dilution was performed transferring 50 µL of the microbial suspension to 450 µL of physiological solution. Then, 10 µL of each suspension was plated (Tryptic Soy agar (TSA) to *S. aureus*, BHI agar to *E. coli*, and SD agar to *C. albicans*). The Petri dishes were incubated for 24 h at

37 °C and then the colonies were counted to determinate the CFU/mL value. The graphics were obtained using GraphPad (GraphPad, San Diego, CA, USA) software (version 8). The experiments were performed in triplicate in three different moments ( $n = 9$ ). A significance level of 0.05 was used in all the statistical tests performed. Minitab<sup>®</sup> Statistical Software 20.3 (Minitab, LLC; State College, PA, USA) was used for statistical analysis.

### 3. Results and Discussion

A complete characterization of the functionalization of CNTs and their dispersion into the PHBV matrix was conducted and has been published in our previous studies [3,22]. A representative scheme of CNT functionalization is shown in Figure 1. Firstly, pristine CNTs were oxidized using nitric acid, and after that, oxidized CNTs, labeled CNT-Ox, were functionalized with GABA, and labeled CNT-GB.

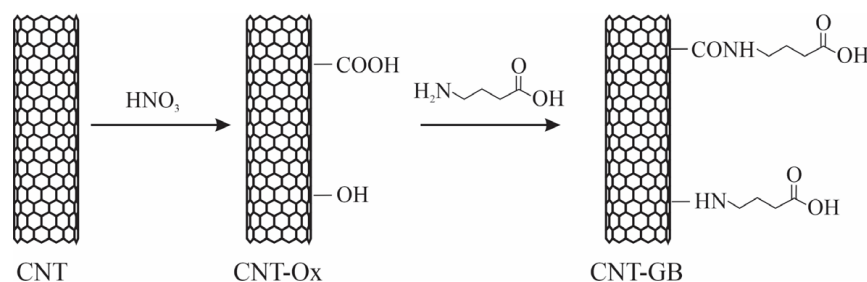


**Figure 1.** Scheme of CNT functionalization.

The MTT assay was performed to evaluate the cytotoxicity of CNT suspensions. Suspensions with different concentrations of CNTs were assessed (1, 5, 10, 50, 100, 500, and 1000  $\mu\text{g/mL}$ ). The suspensions were incubated for 24 h in a DMEM culture medium supplemented with 10% SFB, and the metabolic activity was measured. Figure 2 shows the results.

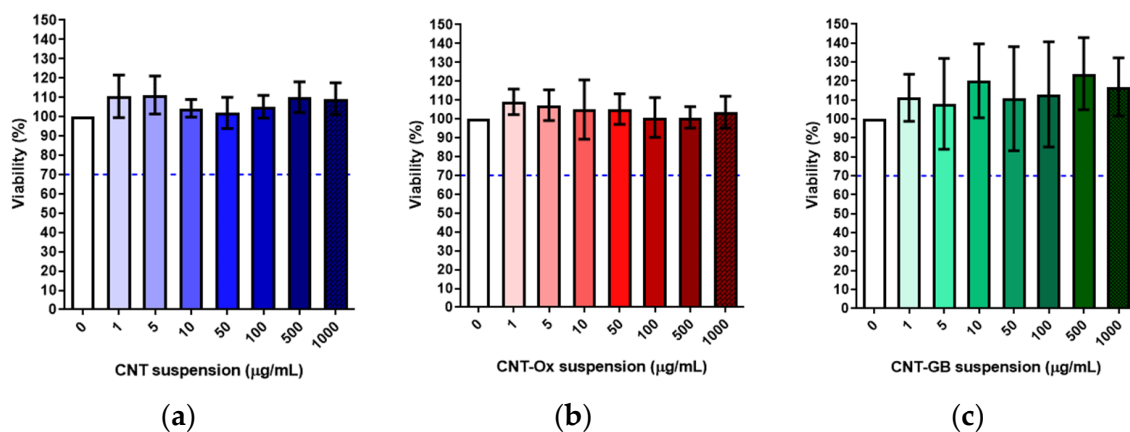


**Figure 2.** Cell viability of (a) CNT (pristine carbon nanotube), (b) CNT-Ox (oxidized CNT), and (c) CNT-GB (GABA-functionalized CNT) suspensions incubated for 24 h in an 80% confluent monolayer.

According to ISO 10993-5, cell viability values greater than 70% are not cytotoxic. So, as shown in Figure 2, all samples can be considered non-toxic for fibroblasts after 24 h of incubation. Even though some values are greater than 100%, statistically all results show similar behaviors. The values presented are the relative viability, with the viability of cells not exposed to nanotubes serving as the control. However, to clarify further, with values exceeding 100% obtained via this methodology, we cannot infer that nanotubes represent promising materials to promote cell proliferation. To make such a statement, further assays would be necessary.

Therefore, to expand the scope of evaluation, new suspensions were tested with concentrations ranging from 100 to 6000  $\mu\text{g/mL}$  over a longer time of incubation. The

suspensions were incubated for 24 h, 4 days, and 6 days. Figures 3–5 show the cell viability results obtained. The 0 mg/mL concentration represents the control, where the cells were incubated only with the culture medium, without sample extracts.

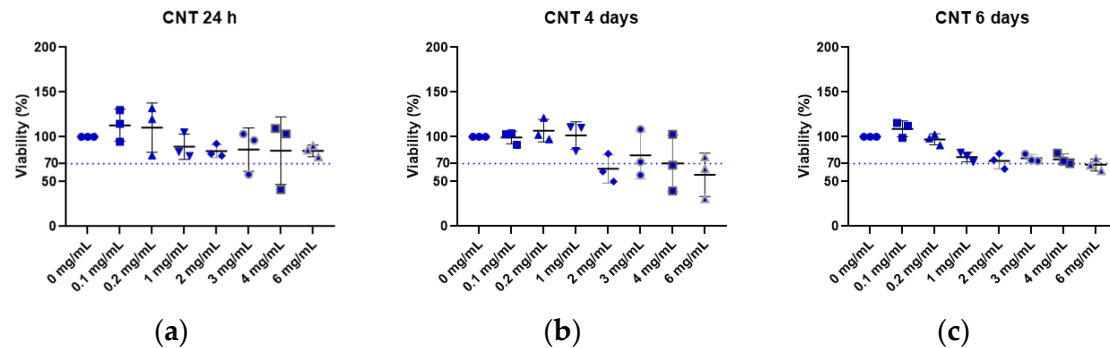


**Figure 3.** Cell viability after contact with (pristine) CNT extract at different concentrations (0–6 mg/mL) for (a) 24 h, (b) 4 and (c) 6 days.

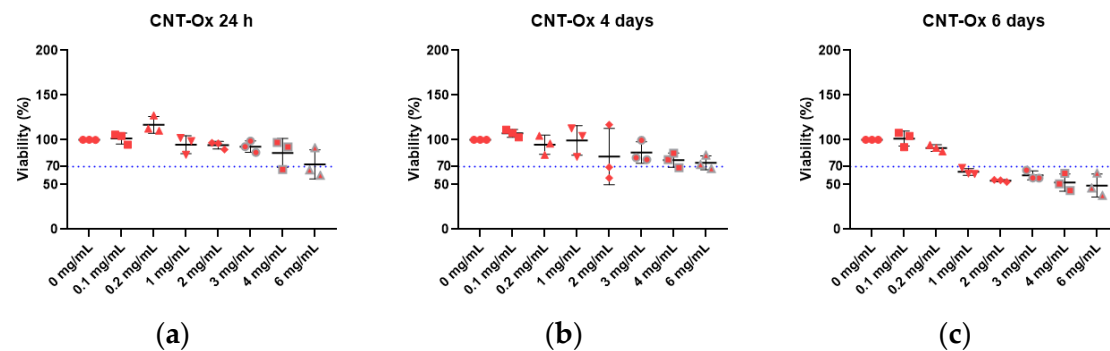


**Figure 4.** Cell viability after contact with CNT-Ox (oxidized CNT) extracts at different concentrations (0–6 mg/mL) for (a) 24 h, (b) 4, and (c) 6 days.

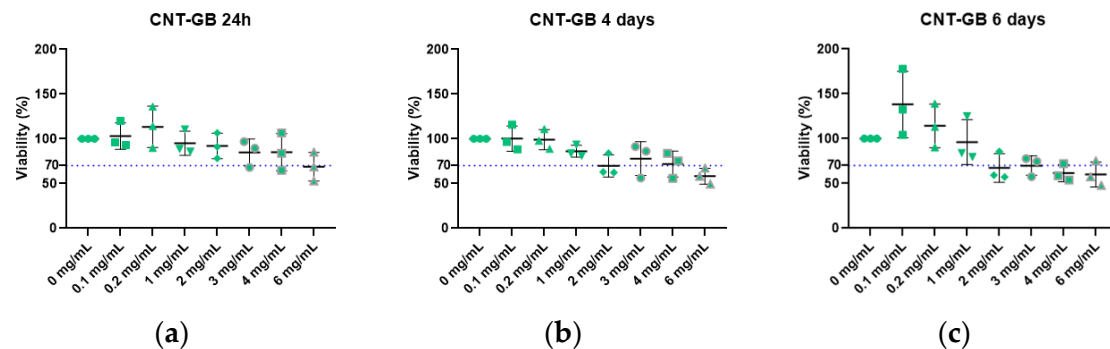


**Figure 5.** Cell viability after contact with CNT-GB (GABA-functionalized) extracts at different concentrations (0–6 mg/mL) for (a) 24 h, (b) 4, and (c) 6 days.

As expected, after a long incubation time and with high concentrations, the cytotoxicity against fibroblasts increased for all samples. CNT cytotoxicity can be influenced by the presence of metallic impurities and the amounts thereof, the length and type of nanotubes, the presence and type of functionalization, and other residues [6]. Gutiérrez-Praena et al. (2011) [40] showed results similar to those obtained above. The authors reported that both single-walled carbon nanotubes (SWCNT) functionalized with carboxylic groups (as in the case of Ox-CNT) and non-functionalized nanotubes induce toxicity in endothelial cells of the human umbilical vein, which is proportional to concentration and time. Furthermore, functionalized SWCNTs have been reported to induce more significant toxicity when compared to non-functionalized ones [40].

The cytotoxicity starts to be more significant after six days, and with concentrations above  $2 \text{ mg}\cdot\text{mL}^{-1}$ . Two-way ANOVA statistics analysis aimed to understand the possible cause of the cytotoxic effect. Figure 6 shows a comparative study between pristine and functionalized samples.

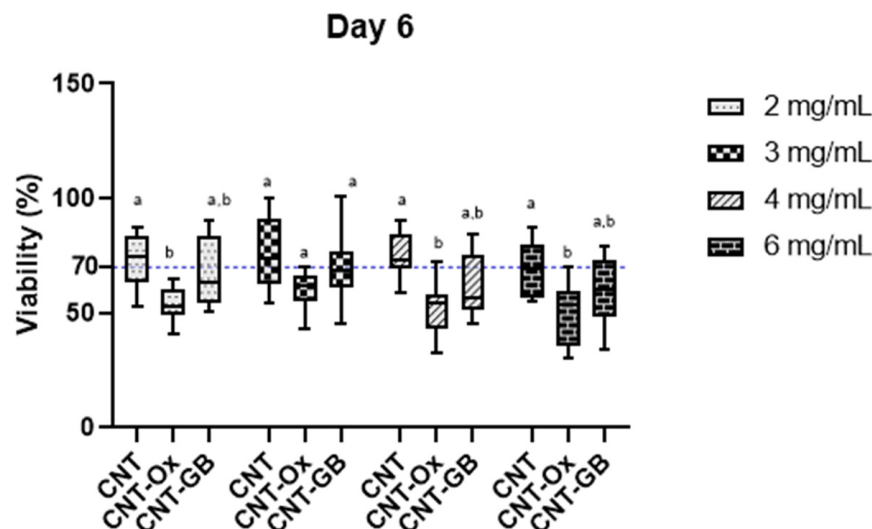


**Figure 6.** Comparison of cell viability percentages after contact with the materials' extract at the concentrations of 2 to 6 mg/mL for 6 days (two-way ANOVA statistical analysis) for CNT (pristine CNT), CNT-Ox (oxidized CNT), and CNT-GB (GABA-functionalized CNT). Different letters (a and b) were used to represent statistical differences.

It is observed that, in all evaluated concentrations, the cellular viabilities of CNT and CNT-GB are not statistically different. Except for the concentration of 2 mg/mL, the cell viability of CNT-Ox was significantly lower than that of CNT. However, it was not different from CNT-GB. Therefore, the oxidation of CNTs can potentially make the nanotubes more cytotoxic than the original without functionalization.

The lower viability obtained for CNT-Ox may be explained by the enhanced uptake into cells, which is related to both endocytosis and passive uptake. In contrast, pristine CNTs did not influence the mitotic pathway, once they formed agglomerates that prevented uptake. These agglomerates were formed due to the relatively hydrophobic surface of pristine CNTs [41].

Mohammadi et al. [42] evaluated the effects of functionalization with amine or carboxylic acid of CNTs on toxicological parameters in mice, and reported that amino-functionalized CNTs showed a higher toxicity than the oxidized ones.

In this study, GABA-functionalized CNTs were evaluated. Despite GABA having amine groups in its structure, this group was covalently attached to the CNT surface, so we cannot expect similar behavior to that seen in the study by Mohammadi et al. [42]. According to the scheme in Figure 1, we can still observe oxygenated groups on the CNT-GB surface, but they are at the end of a four-carbon chain. Therefore, we may hypothesize that CNT-GB would exhibit intermediate cytotoxicity compared to CNT and CNT-Ox, which is consistent with the findings presented in Figure 6.

The evaluated CNT, CNT-OX, and CNT-GB were used to produce nanocomposites with PHBV matrix at 0.5 wt. %. It is widely discussed in the literature that PHBV does not present cytotoxicity for cells [43,44], and recently, it was found that D-3-hydroxybutyric acid, the degradation product of PHBV, is a valuable constituent of human blood [16]. The cytotoxicity exhibited by the extract previously evaluated is not representative of the cytotoxicity of the nanocomposites when CNTs are embedded in the polymer matrix. However, if we confirm that CNTs alone do not exhibit cytotoxicity, it can be inferred that the nanocomposites will also not be cytotoxic. Considering that 0.5% of CNT in

a suspension would be 0.005 g/mL, we can assume that no cytotoxic effects would be observed in the nanocomposites at any of the evaluated times.

#### Antibiofilm Effect of PHBV and CNT Nanocomposites

The antibiofilm effects of the different types of CNTs were assessed. *Escherichia coli* was used as a representative Gram-negative bacterium. *Staphylococcus aureus*, a ubiquitous bacterium, was used to represent the Gram-positive bacteria, and *Candida albicans* was used to represent fungi. These microorganisms were chosen because they are of biomedical interest and commonly used for conducting initial screenings of materials' potential to inhibit biofilm formation [45–48]. After 24 h of incubation, the groups tested did not show a significant difference in the counts of viable cells recovered from the biofilms formed on the nanocomposites ( $p > 0.05$ , Mann–Whitney test) (Figure 7). Gram-positive bacterial cells have a cell wall measuring approximately 20 nm thick, containing a peptidoglycan layer infused with teichoic acids. The total cell wall can reach a thickness of 30–100 nm [49,50]. In contrast, Gram-negative bacteria exhibit distinct characteristics compared to Gram-positive bacteria, with a thinner peptidoglycan layer (3–8 nm) and an additional outer membrane consisting of lipopolysaccharide (1–3  $\mu\text{m}$  thick) [51,52]. So, it was expected that different compositions of the bacterial cell wall and its mechanical characteristics could influence the CNT antibacterial capacity.

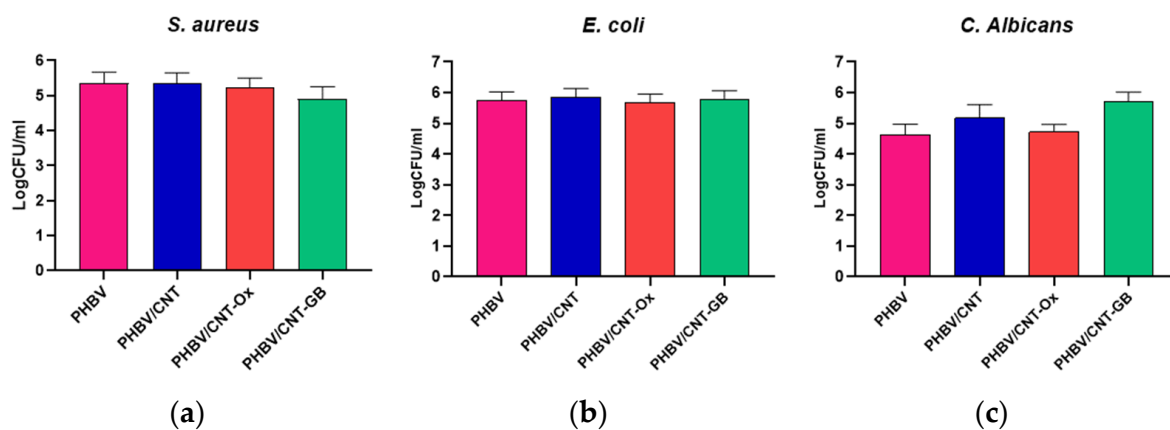


**Figure 7.** Number of colony-forming units per milliliter (CFU/mL) obtained from the specimens of PHBV (neat polymer), PHBV/CNT (PHBV with 0.5 wt. % of pristine CNT), PHBV/CNT-Ox (PHBV with 0.5 wt. % of oxidized CNT), and PHBV/CNT-GB (PHBV with 0.5 wt. % of GABA-functionalized CNT) after 24 h of incubation of with (a) *S. aureus*, (b) *E. coli*, and (c) *C. albicans*.

In this way, the reduction in CFU/mL was calculated concerning the control sample (PHBV) ( $n = 9$ ). It was possible to observe a decrease in the formation of the *S. aureus* biofilm equal to 20 and 64% for the PHBV/NTC-Ox and PHBV/NTC-GB samples, respectively. However, the biofilm formed by *E. coli* was reduced by only 15% in the PHBV/NTC-Ox sample. As mentioned above, Gram-negative bacteria have an external coating formed by a layer of lipopolysaccharides, which functions as an additional barrier inhibiting the penetration of antimicrobial agents. The other samples showed no reduction concerning the control.

Differently from the results of the present study, other studies reported the antimicrobial properties of MWCNTs. Moreover, modified MWCNTs exhibited better antimicrobial properties compared to pristine MWCNTs. This improvement can be attributed to their ability to penetrate through the membranes of microbial cells. Some hypotheses about the mechanism of action of carbon nanotubes in bacteria cells are described in the literature, including oxidative stress and the mechanical interactions of carbon-based nanomaterials.

CNTs are known to have antimicrobial properties; however, for this effect to be practical, considering their presence in a polymer composite, the CNTs must be homogeneously dispersed in the matrix [53]. Therefore, the better the CNTs' dispersion, the better the biofilm formation-inhibition effect.

The amount of CNT dispersed in the matrix is also an important factor to be evaluated. Dong et al. (2012) [54] showed that single-walled carbon nanotubes exhibit antibacterial properties against both *Salmonella enterica* and *Escherichia coli* in a dose-dependent manner, indicating that nanotube concentration is a relevant factor in the antibacterial effect. Vidakis et al. (2021) [55] showed that MWCNTs (5.0 wt. %) in the PLA matrix can introduce antibacterial properties to the polymer. Amounts lower than 5.0 wt. % did not show any antibacterial effect.

In the present study, the composite materials were prepared with a very low concentration of CNTs, and this property may explain the findings. In this way, it can be said that the reductions found in forming biofilms for scientific samples are promising from the point of view of assisting in managing and preventing diseases related to bacterial infection. Previous work showed that CNT functionalized with GABA presents a better dispersion in the PHBV matrix compared to oxidized CNT. So, according to the experimental results compiled in this study, the potential mechanism of inhibition that can help explain the bactericidal ability of the nanocomposites studied is related to the better dispersion of CNT-GB on the PHBV matrix.

To date, only a few studies have shown the potential antifungal activity of CNT. Benincasa et al. (2011) [56] observed that CNTs show antifungal activity when conjugated with the antimycotic drug amphotericin B (AMB), improving its therapeutic activity while decreasing its toxicity. Hadi Zare-Zardini et al. (2012) [57] studied the antifungal activity of pristine and functionalized MWCNTs by arginine and lysine against ten different fungal species, including *Candida albicans*. The results demonstrate an inhibition between 10 and 30% in the antifungal activity.

Considering these previous reports, the opportunistic pathogen *Candida albicans* was used to evaluate the antimycotic effect of the composites. The fungal cell wall is a remarkably complex framework composed of a network of polysaccharides, within which different proteins are twisted [57]. Our results against *Candida albicans* show no significant differences among the studied groups. Unlike the bacteria's prokaryotic cell type, *C. albicans* have eukaryotic cells. There are differences in the cell's internal organization and general structure, such as the two-layered wall, which is primarily composed of carbohydrates and proteins [58]. These characteristics are intrinsically related to the protective and pathogenic aspects [59]. This could be one of the main reasons for a higher antifungal resistance to the nanocomposite activity. Reyes-García et al. [60] studied in vitro the influence of GABA on PLB1 mRNA expression, which is related to virulence factors of *C. albicans*. The upregulation of those factors increased when using GABA, as reflected in the yeast germ-tube formation. The results indicate that germ-tube formation and the GABA concentration increased proportionally. Our results indicate a similar behavior. The PHBV/CNT-GB sample showed a trend of higher biofilm formation than the other groups. Furthermore, the *C. albicans* biofilm was formed due to an initial cell attachment, mainly performed by the yeast adhesins. After the attachment phase, the hyphal and pseudo-hyphal formations play an important role in biofilm development. The expression of many different virulence factors and the extracellular polymeric matrix formation also confer more resistance to the biofilm [61].

As cytotoxicity was shown to be concentration- and time-dependent for CNT, CNT-Ox, and CNT-GB samples, and in the case of antimicrobial evaluation, only 24 h tests were conducted in this study; there is thus room for evaluating longer incubation times, similarly to what was done with the cells, and the material's performance may potentially differ.

#### 4. Conclusions

The cytotoxicity assessment using fibroblasts revealed that all MWCNT suspensions, including pristine, oxidized, and GABA-functionalized, exhibited cell viabilities greater than 70%, indicating non-toxic behavior after 24 h of incubation. Prolonged incubation and higher concentrations increased cytotoxicity, with oxidation potentially enhancing nanotube toxicity. Statistical analysis has indicated that MWCNT and MWCNT-GB samples had similar cellular viabilities, while MWCNT-Ox showed differences, especially at 2 mg/mL. The antibacterial potential of PHBV/CNT nanocomposites against Gram-negative (*E. coli*) and Gram-positive (*S. aureus*) bacteria showed a trend of reducing biofilm formation, with PHBV/CNT-GB outperforming PHBV/CNT-Ox, although it was not statistically significant. Besides this, antifungal activity against *C. albicans* was not significant. The results indicate promising applications for PHBV/CNT nanocomposites in managing bacterial infections, with GABA-functionalized CNTs showing enhanced performance. Further investigations are warranted to explore the potential antifungal properties and optimize composite formulations for specific applications.

**Author Contributions:** Conceptualization, T.L.d.A.M. and G.P.T.; data curation, T.L.d.A.M., V.M.S., D.E.M.C., T.C.d.O. and M.R.d.C.V.; formal analysis, T.L.d.A.M., D.E.M.C., D.M.d.S. and M.R.d.C.V.; funding acquisition, T.L.d.A.M., L.H.C., C.Y.K.-I. and G.P.T.; investigation, T.L.d.A.M., V.M.S. and D.M.d.S.; methodology, T.L.d.A.M., D.E.M.C., D.M.d.S. and M.R.d.C.V.; project administration, T.L.d.A.M.; resources, T.L.d.A.M., L.H.C., C.Y.K.-I. and G.P.T.; software, T.L.d.A.M., D.E.M.C., D.M.d.S. and M.R.d.C.V.; supervision, L.H.C., C.Y.K.-I. and G.P.T.; validation, T.L.d.A.M., L.H.C., C.Y.K.-I. and G.P.T.; visualization, T.L.d.A.M.; writing—original draft, T.L.d.A.M. and V.M.S.; writing—review and editing, T.L.d.A.M., V.M.S., D.E.M.C., T.C.d.O. and D.M.d.S. All authors have read and agreed to the published version of the manuscript.

**Funding:** This research was funded by FUNDAÇÃO DE AMPARO À PESQUISA DO ESTADO DE SÃO PAULO (FAPESP), grant numbers 2017/24873-4, 2011/21442-6, 2020/12507-6, 2019/05856-7, and 2018/13492-2.

**Data Availability Statement:** Data will be made available on request.

**Conflicts of Interest:** The authors declare no conflicts of interest.

#### References

1. de Menezes, B.R.C.; Rodrigues, K.F.; Fonseca, B.C.S.; Ribas, R.G.; Montanheiro, T.L.A.; Thim, G.P. Recent advances in the use of carbon nanotubes as smart biomaterials. *J. Mater. Chem. B* **2019**, *7*, 1343–1360. [[CrossRef](#)] [[PubMed](#)]
2. Montanheiro, T.L.A.; Cristóvan, F.H.; Machado, J.P.B.; Tada, D.B.; Durán, N.; Lemes, A.P. Effect of MWCNT functionalization on thermal and electrical properties of PHBV/MWCNT nanocomposites. *J. Mater. Res.* **2014**, *30*, 55–65. [[CrossRef](#)]
3. Montanheiro, T.L.A.; de Menezes, B.R.C.; Ribas, R.G.; Montagna, L.S.; Campos, T.M.B.; Schatkoski, V.M.; Righetti, V.A.N.; Passador, F.R.; Thim, G.P. Covalently  $\gamma$ -aminobutyric acid-functionalized carbon nanotubes: Improved compatibility with PHBV matrix. *SN Appl. Sci.* **2019**, *1*, 1177. [[CrossRef](#)]
4. Jin, Q.; Zheng, Z.; Feng, Y.; Tian, S.; He, Z. Multi-Walled Carbon Nanotubes Modified NiCo<sub>2</sub>S<sub>4</sub> for the Efficient Photocatalytic Reduction of Hexavalent Chromium. *C* **2023**, *9*, 99. [[CrossRef](#)]
5. Estévez-Martínez, Y.; Quiroga-González, E.; Cuevas-Yañez, E.; Durón-Torres, S.; Alaníz-Lumbreras, D.; Chavira-Martínez, E.; Posada-Gómez, R.; Bravo-Tapia, J.; Castaño-Meneses, V. Membranes of Multiwall Carbon Nanotubes in Chitosan–Starch with Mechanical and Compositional Properties Useful in Li-Ion Batteries. *C* **2023**, *9*, 87. [[CrossRef](#)]
6. Alshehri, R.; Ilyas, A.M.; Hasan, A.; Arnaout, A.; Ahmed, F.; Memic, A. Carbon Nanotubes in Biomedical Applications: Factors, Mechanisms, and Remedies of Toxicity. *J. Med. Chem.* **2016**, *59*, 8149–8167. [[CrossRef](#)]
7. Vardharajula, S.; Ali, S.Z.; Tiwari, P.M.; Eroglu, E.; Vig, K.; Dennis, V.; Singh, S.R. Functionalized carbon nanotubes: Biomedical applications. *Int. J. Nanomed.* **2012**, *7*, 5361–5374. [[CrossRef](#)]
8. Wang, X.; Lim, E.G.; Hoettges, K.; Song, P. A Review of Carbon Nanotubes, Graphene and Nanodiamond Based Strain Sensor in Harsh Environments. *C* **2023**, *9*, 108. [[CrossRef](#)]
9. Träger, D.; Słota, D.; Niziołek, K.; Florkiewicz, W.; Sobczak-Kupiec, A. Hybrid Polymer–Inorganic Coatings Enriched with Carbon Nanotubes on Ti-6Al-4V Alloy for Biomedical Applications. *Coatings* **2023**, *13*, 1813. [[CrossRef](#)]
10. Aoki, K.; Ogihara, N.; Tanaka, M.; Haniu, H.; Saito, N. Carbon nanotube-based biomaterials for orthopaedic applications. *J. Mater. Chem. B* **2020**, *8*, 9227–9238. [[CrossRef](#)]

11. Abdelrazek, E.M.; Hezma, A.M.; El-khodary, A.; Elzayat, A.M.; Rajeh, A. Modifying of Structural, Optical, Thermal, and Mechanical Properties of PCL/PMMA Biomaterial Blend Doped With MWCNTs as an Application in Materials Science. *J. Inorg. Organomet. Polym. Mater.* **2023**, *33*, 4117–4126. [[CrossRef](#)]
12. Neto, J.S.S.; Cavalcanti, D.K.K.; da Cunha Ferro, L.E.; de Queiroz, H.F.M.; Aguiar, R.A.A.; Banea, M.D. Effect of Multi-Walled Carbon Nanotubes on the Mechanical and Thermal Properties of Curauá Natural-Fiber-Reinforced Composites. *C* **2023**, *9*, 102. [[CrossRef](#)]
13. Montanheiro, T.L.A.; Ribas, R.G.; Montagna, L.S.; de Menezes, B.R.C.; Schatkoski, V.M.; Rodrigues, K.F.; Thim, G.P. A brief review concerning the latest advances in the influence of nanoparticle reinforcement into polymeric-matrix biomaterials. *J. Biomater. Sci. Polym. Ed.* **2020**, *31*, 1869–1893. [[CrossRef](#)] [[PubMed](#)]
14. Loura, N.; Gkartzou, E.; Trompeta, A.-F.; Konstantopoulos, G.; Klonos, P.A.; Kyritsis, A.; Charitidis, C.A. Development of CNT-Based Nanocomposites with Ohmic Heating Capability towards Self-Healing Applications in Extrusion-Based 3D Printing Technologies. *C* **2023**, *9*, 111. [[CrossRef](#)]
15. Lemes, A.P.; Montanheiro, T.L.A.; da Silva, A.P.; Durán, N. PHBV/MWCNT Films: Hydrophobicity, Thermal and Mechanical Properties as a Function of MWCNT Concentration. *J. Compos. Sci.* **2019**, *3*, 12. [[CrossRef](#)]
16. Wang, Q.; Ma, J.; Chen, S.; Wu, S. Designing an Innovative Electrospinning Strategy to Generate PHBV Nanofiber Scaffolds with a Radially Oriented Fibrous Pattern. *Nanomaterials* **2023**, *13*, 1150. [[CrossRef](#)] [[PubMed](#)]
17. Rodríguez-Cendal, A.I.; Gómez-Seoane, I.; de Toro-Santos, F.J.; Fuentes-Boquete, I.M.; Señaris-Rodríguez, J.; Díaz-Prado, S.M. Biomedical Applications of the Biopolymer Poly(3-hydroxybutyrate-co-3-hydroxyvalerate) (PHBV): Drug Encapsulation and Scaffold Fabrication. *Int. J. Mol. Sci.* **2023**, *24*, 11674. [[CrossRef](#)]
18. Butron, A.; Llorente, O.; Fernandez, J.; Meaurio, E.; Sarasua, J.R. Morphology and mechanical properties of poly(ethylene brassylate)/cellulose nanocrystal composites. *Carbohydr. Polym.* **2019**, *221*, 137–145. [[CrossRef](#)] [[PubMed](#)]
19. Montanheiro, T.L.A.; Montagna, L.S.; Patrúlea, V.; Jordan, O.; Borchard, G.; Ribas, R.G.; Campos, T.M.B.; Thim, G.P.; Lemes, A.P. Enhanced water uptake of PHBV scaffolds with functionalized cellulose nanocrystals. *Polym. Test.* **2019**, *79*, 106079. [[CrossRef](#)]
20. Montanheiro, T.L.A.; Montagna, L.S.; Patrúlea, V.; Jordan, O.; Borchard, G.; Lobato, G.M.M.; Catalani, L.H.; Lemes, A.P. Evaluation of cellulose nanocrystal addition on morphology, compression modulus and cytotoxicity of poly (3-hydroxybutyrate-co -3-hydroxyvalerate) scaffolds. *J. Mater. Sci. Mater. life Sci.* **2019**, *54*, 7198–7210. [[CrossRef](#)]
21. Montanheiro, T.L.A.; Campos, T.M.B.; Montagna, L.S.S.; da Silva, A.P.; Ribas, R.G.; de Menezes, B.R.C.; Passador, F.R.; Thim, G. Influence of CNT pre-dispersion into PHBV/CNT nanocomposites and evaluation of morphological, mechanical and crystallographic features. *Mater. Res. Express* **2019**, *6*, 105375. [[CrossRef](#)]
22. Montanheiro, T.L.A.; de Menezes, B.R.C.; Montagna, L.S.; Beatrice, C.A.G.; Marini, J.; Lemes, A.P.; Thim, G.P. Non-Isothermal Crystallization Kinetics of Injection Grade PHBV and PHBV/Carbon Nanotubes Nanocomposites Using Isoconversional Method. *J. Compos. Sci.* **2020**, *4*, 52. [[CrossRef](#)]
23. Silva, A.P.; Amaral Montanheiro, T.L.; Stieven Montagna, L.; Andrade, P.F.; Durán, N.; Lemes, A.P. Effect of carbon nanotubes on the biodegradability of poly(3-hydroxybutyrate-co-3-hydroxyvalerate) nanocomposites. *J. Appl. Polym. Sci.* **2019**, *48020*, 48020. [[CrossRef](#)]
24. Montagna, L.S.; Oyama, I.C.; Lamparelli, R.C.B.C.; Da Silva, A.P.; Montanheiro, T.L.A.; Lemes, A.P. Evaluation of Biodegradation in Aqueous Medium of Poly(Hydroxybutyrate-Co-Hydroxyvalerate)/Carbon Nanotubes Films in Respirometric System. *J. Renew. Mater.* **2019**, *7*, 117–128. [[CrossRef](#)]
25. Song, Y.; Lin, K.; He, S.; Wang, C.; Zhang, S.; Li, D.; Wang, J.; Cao, T.; Bi, L.; Pei, G. Nano-biphasic calcium phosphate / polyvinyl alcohol composites with enhanced bioactivity for bone repair via low-temperature three-dimensional printing and loading with platelet-rich fibrin. *J. Nanomed.* **2018**, *13*, 505–523. [[CrossRef](#)] [[PubMed](#)]
26. Molaei, A.; Yousefpour, M. Electrophoretic deposition of chitosan–bioglass®–hydroxyapatite–halloysite nanotube composite coating. *Rare Met.* **2022**, *41*, 3850–3857. [[CrossRef](#)]
27. Azizi-Lalabadi, M.; Hashemi, H.; Feng, J.; Jafari, S.M. Carbon nanomaterials against pathogens; the antimicrobial activity of carbon nanotubes, graphene/graphene oxide, fullerenes, and their nanocomposites. *Adv. Colloid Interface Sci.* **2020**, *284*, 102250. [[CrossRef](#)] [[PubMed](#)]
28. Ansari, S.; Sami, N.; Yasin, D.; Ahmad, N.; Fatma, T. Biomedical applications of environmental friendly poly-hydroxyalkanoates. *Int. J. Biol. Macromol.* **2021**, *183*, 549–563. [[CrossRef](#)] [[PubMed](#)]
29. Răpă, M.; Stefan, L.M.; Seciu-Grama, A.-M.; Gaspar-Pintilieșcu, A.; Matei, E.; Zaharia, C.; Stănescu, P.O.; Predescu, C. Poly(3-hydroxybutyrate-co-3-hydroxyvalerate) (P(3HB-co-3HV))/Bacterial Cellulose (BC) Biocomposites for Potential Use in Biomedical Applications. *Polymers* **2022**, *14*, 5544. [[CrossRef](#)]
30. Shah, A.A.; Hasan, F.; Hameed, A.; Ahmed, S. Biological degradation of plastics: A comprehensive review. *Biotechnol. Adv.* **2008**, *26*, 246–265. [[CrossRef](#)]
31. Sivan, A. New perspectives in plastic biodegradation. *Curr. Opin. Biotechnol.* **2011**, *22*, 422–426. [[CrossRef](#)]
32. Bustamante-Torres, M.; Arcentales-Vera, B.; Estrella-Nuñez, J.; Yáñez-Vega, H.; Bucio, E. Antimicrobial Activity of Composites-Based on Biopolymers. *Macromol* **2022**, *2*, 258–283. [[CrossRef](#)]
33. Vagos, M.R.; Gomes, M.; Moreira, J.M.R.; Soares, O.S.G.P.; Pereira, M.F.R.; Mergulhão, F.J. Carbon nanotube/poly(Dimethylsiloxane) composite materials to reduce bacterial adhesion. *Antibiotics* **2020**, *9*, 434. [[CrossRef](#)]

34. Goodwin, D.G.; Marsh, K.M.; Sosa, I.B.; Payne, J.B.; Gorham, J.M.; Bouwer, E.J.; Fairbrother, D.H. Interactions of Microorganisms with Polymer Nanocomposite Surfaces Containing Oxidized Carbon Nanotubes. *Environ. Sci. Technol.* **2015**, *49*, 5484–5492. [[CrossRef](#)]
35. Mohammed, M.K.A.; Mohammad, M.R.; Jabir, M.S.; Ahmed, D.S. Functionalization, characterization, and antibacterial activity of single wall and multi wall carbon nanotubes. *IOP Conf. Ser. Mater. Sci. Eng.* **2020**, *757*, 012028. [[CrossRef](#)]
36. Talodthaisong, C.; Plaeyao, K.; Mongseetong, C.; Boonta, W.; Srichaiyapol, O.; Patramanon, R.; Kayunkid, N.; Kulchat, S. The Decoration of ZnO Nanoparticles by Gamma Aminobutyric Acid, Curcumin Derivative and Silver Nanoparticles: Synthesis, Characterization and Antibacterial Evaluation. *Nanomaterials* **2021**, *11*, 442. [[CrossRef](#)]
37. Yurtdaş Kırımlıoğlu, G.; Menciloğlu, Y.; Erol, K.; Yazan, Y. In vitro/in vivo evaluation of gamma-aminobutyric acid-loaded N, N -dimethylacrylamide-based pegylated polymeric nanoparticles for brain delivery to treat epilepsy. *J. Microencapsul.* **2016**, *33*, 625–635. [[CrossRef](#)]
38. Immich, A.P.S.; Pennacchi, P.C.; Naves, A.F.; Felisbino, S.L.; Boemo, R.L.; Maria-Engler, S.S.; Catalani, L.H. Improved tympanic membrane regeneration after myringoplastic surgery using an artificial biograft. *Mater. Sci. Eng. C* **2017**, *73*, 48–58. [[CrossRef](#)] [[PubMed](#)]
39. ISO/EN10993-5; International Standard ISO 10993-5 Biological Evaluation of Medical Devices: Tests for In Vitro Cytotoxicity. Part 5 Tests Cytotox. *Vitr. Methods*; ISO: Genève, Switzerland, 2009.
40. Gutiérrez-Praena, D.; Pichardo, S.; Sánchez, E.; Grilo, A.; Cameán, A.M.; Jos, A. Influence of carboxylic acid functionalization on the cytotoxic effects induced by single wall carbon nanotubes on human endothelial cells (HUVEC). *Toxicol. Vitr.* **2011**, *25*, 1883–1888. [[CrossRef](#)]
41. Fraczek-Szczypta, A.; Menaszek, E.; Syeda, T.B.; Misra, A.; Alavijeh, M.; Adu, J.; Blazewicz, S. Effect of MWCNT surface and chemical modification on in vitro cellular response. *J. Nanoparticle Res.* **2012**, *14*, 1181. [[CrossRef](#)]
42. Mohammadi, E.; Zeinali, M.; Mohammadi-Sardoo, M.; Iranpour, M.; Behnam, B.; Mandegary, A. The effects of functionalization of carbon nanotubes on toxicological parameters in mice. *Hum. Exp. Toxicol.* **2020**, *39*, 1147–1167. [[CrossRef](#)]
43. Malmir, S.; Barral, L.; Bouza, R.; Esperanza, M.; Seoane, M.; Feijoo-Bandín, S.; Lago, F. Poly (3-hydroxybutyrate-co-3-hydroxyvalerate)/cellulose nanocrystal films: Artificial weathering, humidity absorption, water vapor transmission rate, antimicrobial activity and biocompatibility. *Cellulose* **2019**, *26*, 2333–2348. [[CrossRef](#)]
44. Braga, N.F.; Vital, D.A.; Guerrini, L.M.; Lemes, A.P.; Formaggio, D.M.D.; Tada, D.B.; Arantes, T.M.; Cristovan, F.H. PHBV-TiO<sub>2</sub> mats prepared by electrospinning technique: Physico-chemical properties and cytocompatibility. *Biopolymers* **2018**, *109*, e23120. [[CrossRef](#)]
45. Piedade, A.P.; Pinho, A.C.; Branco, R.; Morais, P.V. Evaluation of antimicrobial activity of ZnO based nanocomposites for the coating of non-critical equipment in medical-care facilities. *Appl. Surf. Sci.* **2020**, *513*, 145818. [[CrossRef](#)]
46. Singh, V.K.; Kumari, P.; Som, A.; Rai, S.; Mishra, R.; Singh, R.K. Design, synthesis and antimicrobial activity of novel quinoline derivatives: An in silico and in vitro study. *J. Biomol. Struct. Dyn.* **2023**, 1–21, *online ahead of print*. [[CrossRef](#)] [[PubMed](#)]
47. Mohamed, E.A.A.; Muddathir, A.M.; Osman, M.A. Antimicrobial activity, phytochemical screening of crude extracts, and essential oils constituents of two *Pulicaria* spp. growing in Sudan. *Sci. Rep.* **2020**, *10*, 17148. [[CrossRef](#)]
48. Anandhi, S.; Leo Edward, M.; Jaisankar, V. Synthesis, characterization and antimicrobial activity of polyindole/ZrO<sub>2</sub> nanocomposites. *Mater. Today Proc.* **2021**, *40*, S93–S101. [[CrossRef](#)]
49. Rohde, M. The Gram-Positive Bacterial Cell Wall. *Microbiol. Spectr.* **2019**, *7*. [[CrossRef](#)]
50. Pasquina-Lemonche, L.; Burns, J.; Turner, R.D.; Kumar, S.; Tank, R.; Mullin, N.; Wilson, J.S.; Chakrabarti, B.; Bullough, P.A.; Foster, S.J.; et al. The architecture of the Gram-positive bacterial cell wall. *Nature* **2020**, *582*, 294–297. [[CrossRef](#)]
51. Mai-Prochnow, A.; Clauson, M.; Hong, J.; Murphy, A.B. Gram positive and Gram negative bacteria differ in their sensitivity to cold plasma. *Sci. Rep.* **2016**, *6*, 38610. [[CrossRef](#)]
52. Slavin, Y.N.; Asnis, J.; Häfeli, U.O.; Bach, H. Metal nanoparticles: Understanding the mechanisms behind antibacterial activity. *J. Nanobiotechnology* **2017**, *15*, 65. [[CrossRef](#)] [[PubMed](#)]
53. Kim, K.I.; Kim, D.A.; Patel, K.D.; Shin, U.S.; Kim, H.W.; Lee, J.H.; Lee, H.H. Carbon nanotube incorporation in PMMA to prevent microbial adhesion. *Sci. Rep.* **2019**, *9*, 4921. [[CrossRef](#)]
54. Dong, L.; Henderson, A.; Field, C. Antimicrobial Activity of Single-Walled Carbon Nanotubes Suspended in Different Surfactants. *J. Nanotechnol.* **2012**, *2012*, 928924. [[CrossRef](#)]
55. Vidakis, N.; Petousis, M.; Kourinou, M.; Velidakis, E.; Mountakis, N.; Fischer-Griffiths, P.E.; Grammatikos, S.; Tzounis, L. Additive manufacturing of multifunctional polylactic acid (PLA)—Multiwalled carbon nanotubes (MWCNTs) nanocomposites. *Nanocomposites* **2021**, *7*, 184–199. [[CrossRef](#)]
56. Benincasa, M.; Pacor, S.; Wu, W.; Prato, M.; Bianco, A.; Gennaro, R. Antifungal Activity of Amphotericin B Conjugated to Carbon Nanotubes. *ACS Nano* **2011**, *5*, 199–208. [[CrossRef](#)] [[PubMed](#)]
57. Zare-Zardini, H.; Amiri, A.; Shanbedi, M.; Memarpoor-Yazdi, M.; Asoodeh, A. Studying of antifungal activity of functionalized multiwalled carbon nanotubes by microwave-assisted technique. *Surf. Interface Anal.* **2013**, *45*, 751–755. [[CrossRef](#)]
58. David, M.E.; Ion, R.-M.; Grigorescu, R.M.; Iancu, L.; Holban, A.M.; Nicoara, A.I.; Alexandrescu, E.; Somoghi, R.; Ganciarov, M.; Vasilievici, G.; et al. Hybrid Materials Based on Multi-Walled Carbon Nanotubes and Nanoparticles with Antimicrobial Properties. *Nanomaterials* **2021**, *11*, 1415. [[CrossRef](#)] [[PubMed](#)]

59. McCall, A.D.; Pathirana, R.U.; Prabhakar, A.; Cullen, P.J.; Edgerton, M. Candida albicans biofilm development is governed by cooperative attachment and adhesion maintenance proteins. *npj Biofilms Microbiomes* **2019**, *5*, 21. [[CrossRef](#)] [[PubMed](#)]
60. Reyes-García, M.G.; Hernández-Hernández, F.; García-Tamayo, F. Gamma-aminobutyric acid (GABA) increases in vitro germ-tube formation and phospholipase B1 mRNA expression in Candida albicans. *Mycoscience* **2012**, *53*, 36–39. [[CrossRef](#)]
61. Chen, H.; Zhou, X.; Ren, B.; Cheng, L. The regulation of hyphae growth in Candida albicans. *Virulence* **2020**, *11*, 337–348. [[CrossRef](#)]

**Disclaimer/Publisher's Note:** The statements, opinions and data contained in all publications are solely those of the individual author(s) and contributor(s) and not of MDPI and/or the editor(s). MDPI and/or the editor(s) disclaim responsibility for any injury to people or property resulting from any ideas, methods, instructions or products referred to in the content.